

A Simple Single RF-Chain Multi-Antenna Full-Duplex Relay Can Outperform An Intelligent Reflecting Surface

Armin Bazrafkan, Marija Poposka, Zoran Hadzi-Velkov, and Nikola Zlatanov

Abstract—In this paper, we propose a single RF-chain multi-antenna full-duplex (FD) relay build with b -bit analog phase shifters. Assuming only passive self-interference cancellation at the FD relay, we derive the achievable data rate of a system comprised of a source, the proposed FD relay, and a destination. Next, we compare the data rate of the proposed FD relaying system with the data rate of the same system but with the FD relay replaced by an ideal intelligent reflecting surface (IRS). Our results show that the relaying system with 2-bit quantized analog phase shifters can significantly outperform the IRS system.

I. INTRODUCTION

To meet the ever growing demands for wider bandwidths, the emerging wireless communication standards must use higher frequency bands, such as the millimetre (mmWave, 30–100 GHz) and the sub-millimetre (above 100 GHz) bands. Wireless transmissions in these bands typically necessitates a direct line-of-sight (LoS) between the transmitter and the receiver or an intermediary device with a LoS to both the transmitter and the receiver. The intermediary device may be a conventional relay or a recent alternative known as an intelligent reflecting surface (IRS) [1], [2]. An IRS is an electronic surface comprised of reflecting antenna elements, where each element can reflect the incoming electromagnetic wave by changing its phase shift. Thereby, the IRS can beamform the incoming signal towards a desired direction. In that sense, the IRS resembles a full-duplex (FD) amplify-and-forward relay with a large planar array of antenna elements.

The recent influx of research papers on IRS-aided communications is attributed to the perceived advantages of this technology over conventional relaying [3]. However, although this perception is valid for half-duplex (HD) relaying, as shown in [4], [5], it is yet unclear whether it is also valid for a practical FD relay. Certainly, this perception is not valid for an ideal FD relay that exhibits zero self-interference and has the same number of antenna elements as the IRS. However, an ideal FD relay is impractical to build in the real-world since it would require the same number of RF-chains as the number of antenna elements and a sophisticated self-interference cancellation hardware. Still it remains unclear whether an IRS is able to outperform a practical FD relay, with the same number of antennas as the IRS, but build only with one RF-chain

A. Bazrafkan and N. Zlatanov are with the Department of Electrical and Computer Systems Engineering, Monash University, Melbourne, VIC, Australia. E-mails: (armin.bazrafkan, nikola.zlatanov)@monash.edu

M. Poposka and Z. Hadzi-Velkov are with the Faculty of Electrical Engineering and Information Technologies, Ss. Cyril and Methodius University, 1000 Skopje, Macedonia. E-mails: (poposka, zoranhv)@feit.ukim.edu.mk.

per transmit- and receive-side¹? The aim of this paper is to answer this question. To the best of authors' knowledge, the performance of a single RF-chain multi-antenna FD relay has not been compared to the performance of an IRS yet.

Single RF-chain massive antenna arrays can be implemented by networks of analog phase shifters and have low cost, low complexity, and low power consumption [6], [7]. In fact, analog beamforming is already implemented in Wireless HD and IEEE 802.11ad products.

In this paper, we first propose a simple single RF-chain multi-antenna FD relay implemented with b -bit analog phase shifters, where different antennas are used for transmission and reception, and with passive self-interference cancellation. Next, we derive an achievable data rate when the proposed FD relay is employed to relay the signal between a source and a destination. Then, we compare the data rate of the proposed FD relaying system with the data rate of the same system but with the FD relay replaced by an IRS. Our results show that the relaying system with 2-bit quantized analog phase shifters can significantly outperform the IRS system.

This paper is organized as follows. In Sec. II, we outline the system model and derive a corresponding achievable rate in Sec. III. We provide numerical examples in Sec. IV and finally conclude the paper in Sec. V.

II. SYSTEM MODEL

In the following, we describe the considered communications system model, the channel models, the system design of the proposed FD relay, and the self-interference model.

A. System and Channel Models

We consider a communications system comprised of a single-antenna transmitter, referred to as the *source* and denoted by S , a single-antenna receiver, referred to as the *destination* and denoted by D , and a multi-antenna FD relay denoted by R . We assume that the source and the destination cannot communicate directly due to a physical obstacle that blocks the LoS. Next, we assume that the relay has a LoS to both the source and the destination, and thereby can relay source's signal to the destination. We assume that the relay is equipped with K antennas such that M antennas are used for reception and N antennas are used for transmission, where $M + N = K$.

Let the channel between the source and the m -th receive antenna at the relay be denoted by $h_{SR,m}$. Moreover, let the

¹One RF-chain for the receive-side and one RF-chain for the transmit-side of the FD relay.

channel between the n -th transmit antenna at the relay and the destination be denoted by $h_{RD,n}$. Due to the LoS assumption, $h_{SR,m}$ and $h_{RD,n}$ can be expressed as

$$h_{SR,m} = \sqrt{\Omega_{SR,m}} e^{j\phi_{SR,m}}, \quad (1)$$

$$h_{RD,n} = \sqrt{\Omega_{RD,n}} e^{j\phi_{RD,n}}, \quad (2)$$

where $\Omega_{SR,m}$ and $\Omega_{RD,n}$ are the fixed channel gains between the source and the m -th receive antenna at the relay and between the n -th transmit antenna at the relay and the destination, respectively, which can be found by [8, Lemma 1]. Moreover, $\phi_{SR,m}$ and $\phi_{RD,n}$ are the fixed channel phases between the source and the m -th receive antenna at the relay and between the n -th transmit antenna at the relay and the destination, respectively, determined by the corresponding propagation delays. Thus, the overall channel between the source and the relay can be represented by the vector $\mathbf{h}_{SR} = [h_{SR,1}, h_{SR,2} \dots, h_{SR,M}]^T$. Similarly, the overall channel between relay and the destination can be represented by the vector $\mathbf{h}_{RD} = [h_{RD,1}, h_{RD,2} \dots, h_{RD,N}]^T$.

Let A denote the area of each transmit and receive antenna at the relay. Moreover, let d_{SR} and d_{RD} denote the distance between the source and the centre of the relay's receive antenna array and between the centre of the relay's transmit antenna array and the destination, respectively. Now, if the following conditions hold $\sqrt{MA} \leq 3d_{SR}$ and $\sqrt{NA} \leq 3d_{RD}$, then the source and the destination are located in the far-field region of the relay [8, Eq. (11)]. In that case, $\Omega_{SR,m}$ and $\Omega_{RD,n}$ can be accurately approximated as (c.f. [8, Eq. (31)])

$$\Omega_{SR,m} = \Omega_{SR} = \frac{A \cos(\alpha_{SR})}{4\pi d_{SR}^2}, \quad \forall m, \quad (3)$$

$$\Omega_{RD,n} = \Omega_{RD} = \frac{A \cos(\alpha_{RD})}{4\pi d_{RD}^2}, \quad \forall n, \quad (4)$$

where α_{SR} and α_{RD} are the angles of arrival and departure at the relay with respect to the source and destination, respectively.

In the remainder of the paper, we assume that the source and the destination are located in the far-field region of the relay.

Finally, let $\mathbf{w}_R = [w_{R,1}, w_{R,2}, \dots, w_{R,M}]^T$ denote the additive white Gaussian noise (AWGN) vector at the relay, where $w_{R,m} \sim \mathcal{CN}(0, N_0)$, for $m = 1, \dots, M$, is the AWGN at the m -th receive antenna of the relay. Moreover, let $\mathbf{w}_D \sim \mathcal{CN}(0, N_0)$ denote the AWGN at the destination.

B. The Relay Model

The structure of the proposed FD relay is illustrated in Fig. 1. Thereby, the receive-side of the FD relay is comprised of M antennas, each connected to a b -bit analog phase shifter. The b -bit analog phase shifter can shift the phase of the received signal at the given antenna by a phase from the following set

$$\mathcal{P} = \left\{ 0, \frac{2\pi}{2^b}, 2 \times \frac{2\pi}{2^b}, 3 \times \frac{2\pi}{2^b}, \dots, (2^b - 1) \times \frac{2\pi}{2^b} \right\}. \quad (5)$$

Next, the phase-shifted signals from each receive antenna are summed and send to an RF-chain. The RF-chain obtains a

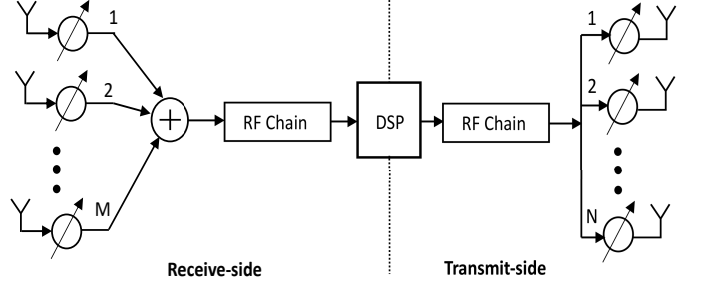


Fig. 1. The relay model.

baseband digital representation of the input signal to the RF-chain, which is then digitally processed.

On the transmit-side of the FD relay, a single RF-chain produces a passband signal which is fed into N transmit antennas. Each transmit antenna is equipped with a b -bit analog phase shifter which shifts the phase of the transmit signal at a given transmit antenna by a phase from the set \mathcal{P} given by (5).

The design in Fig. 1 is a fairly standard hardware design of massive antenna array systems with analog beamforming [6], [7]. In practice, the analog combiner and beamformer with large number of inputs/outputs can be realized as phased arrays (i.e., banks of analog phase shifters) [9], or as "holographic" beamformers [10], [11].

C. Self-Interference

Let g_{mn} denote the self-interference channel between the n -th transmit antenna and the m -th receive antenna at the relay. As shown in [12], the worst-case scenario with respect to the capacity of the given system is when g_{mn} is a zero-mean independent and identically distributed (i.i.d.) Gaussian random variable. In this paper, we assume the worst-case scenario and as a result assume that $g_{mn} \sim \mathcal{CN}(0, \sigma_I^2)$, where σ_I^2 is the power gain of the self-interference channel between the m -th transmit antenna and the n -th receive antenna at the relay. Finally, let \mathbf{G} be a matrix that represents the overall self-interference channel at the relay given by $\mathbf{G} = [g_{mn}]_{M \times N}$.

In the following, we obtain an upper bound on σ_I^2 .

Lemma 1. *In the absence of passive self-interference cancellation at the relay, the power gain of the self-interference channel between any transmit antenna and any receive antenna at the relay, σ_I^2 , must satisfy*

$$\sigma_I^2 \leq \frac{1}{M}. \quad (6)$$

Proof. Assuming that the relay transmits with power P_R , which is equally distributed among the N transmit antennas, the average received power at the relay due to self-interference, denoted by P_I , is given by

$$P_I = \frac{P_R}{N} E \left\{ \left| \sum_{m=1}^M \sum_{n=1}^N g_{mn} \right|^2 \right\} = \frac{P_R}{N} MN \sigma_I^2 = MP_R \sigma_I^2. \quad (7)$$

Due to the law of conservation of energy, the average received power at the relay due to self-interference, P_I , must be smaller or equal to the relay's transmit power P_R , i.e., $P_I \leq P_R$ must hold. As a result, by combining (7) with $P_I \leq P_R$, we obtain (6). \square

Next, we assume that the receive-side and the transmit-side of the relay are passively isolated with a coefficient of passive isolation η . For example, standard passive isolations can reduce the self-interference between 50 dB to 60 dB, making η to take values between 10^{-5} to 10^{-6} , see [13], [14]. Combining the passive isolation with Lemma 1, we obtain that the power gain of the self-interference channel between any transmit antenna and any receive antenna at the relay, σ_I^2 , must satisfy

$$\sigma_I^2 \leq \frac{\eta}{M}. \quad (8)$$

In the rest of the paper, we assume the maximum possible self-interference at the proposed FD relay with passive self-interference cancellation by setting $\sigma_I^2 = \frac{\eta}{M}$, which leads to the smallest possible achievable rate of the considered relaying system.

III. AN ACHIEVABLE RATE

Let x_S denote the signal transmitted by the source such that $E\{|x_S|^2\} = P_S$, where P_S is the transmit power of the source. Let $\bar{y}_{R,m}$ denote the received signal at the m -th receive antenna of the relay before the phase shift is applied and let $\bar{\mathbf{y}}_R = [\bar{y}_{R,1}, \bar{y}_{R,2}, \dots, \bar{y}_{R,M}]^T$. The received vector $\bar{\mathbf{y}}_R$ is comprised of three components: the signal from the source that arrives via the channel \mathbf{h}_{SR} , given by $x_S \mathbf{h}_{SR}$, the noise vector at the relay, \mathbf{w}_R , and the self-interference vector, which is found in the following.

Let $x_R v_n / \sqrt{N}$ denote the transmit signal from the n -th transmit antenna at the relay, where x_R is the information bearing signal of the relay and $v_n \in \mathcal{P}$ is the applied phase shift at the n -th transmit antenna of the relay. Note that when $E\{|x_R|^2\} = P_R$ holds, the transmitted power from the n -th transmit antenna of the relay is P_R/N and the overall transmit power of the relay is P_R . Moreover, let $\mathbf{v} = [v_1, v_2, \dots, v_N]^T$ denote the vector of phase shifts at the transmit antennas of the relay. Then, the self-interference vector at the relay is given by $x_R \mathbf{G} \mathbf{v} / \sqrt{N}$. Combining the three components of $\bar{\mathbf{y}}_R$, we can obtain $\bar{\mathbf{y}}_R$ as

$$\bar{\mathbf{y}}_R = x_S \mathbf{h}_{SR} + \frac{1}{\sqrt{N}} x_R \mathbf{G} \mathbf{v} + \mathbf{w}_R. \quad (9)$$

Next, let $u_m \in \mathcal{P}$ denote the phase shift at the m -th receive antenna of the relay and let $\mathbf{u} = [u_1, u_2, \dots, u_M]^T$ be the receive phase shift vector. Then, the input signal to the receive RF-chain of the relay, which is then digitalized into a digital received symbol, is given by

$$\begin{aligned} y_R &= \mathbf{u}^T \bar{\mathbf{y}}_R \\ &= x_S \mathbf{u}^T \mathbf{h}_S + \frac{1}{\sqrt{N}} x_R \mathbf{u}^T \mathbf{G} \mathbf{v} + \mathbf{u}^T \mathbf{w}_R. \end{aligned} \quad (10)$$

On the other hand, the received symbol at the destination is given by

$$y_D = \frac{1}{\sqrt{N}} x_R \mathbf{v}^T \mathbf{h}_D + w_D, \quad (11)$$

where w_D is the AWGN at the destination.

Theorem 1. *When the phase shift vectors \mathbf{u} and \mathbf{v} are given by*

$$\mathbf{u} = [e^{-j\hat{\phi}_{SR,1}}, e^{-j\hat{\phi}_{SR,2}}, \dots, e^{-j\hat{\phi}_{SR,M}}]^T \quad (12)$$

$$\mathbf{v} = [e^{-j\hat{\phi}_{RD,1}}, e^{-j\hat{\phi}_{RD,2}}, \dots, e^{-j\hat{\phi}_{RD,N}}]^T, \quad (13)$$

where $\hat{\phi}_{SR,n}$ and $\hat{\phi}_{RD,n}$ are the b -bit quantized versions of $\phi_{SR,n}$ and $\phi_{RD,n}$, then the achieved rate is given by

$$R \approx \min \left\{ \log_2 \left(1 + \frac{P_S \Omega_{SR} (1 + (M-1)Q)}{N_0 + \frac{\eta}{M} P_R} \right), \log_2 \left(1 + \frac{P_R \Omega_{RD} (1 + (N-1)Q)}{N_0} \right) \right\}, \quad (14)$$

where

$$Q = \left(\frac{2^b}{\pi} \sin \left(\frac{\pi}{2^b} \right) \right)^2. \quad (15)$$

Proof. Please refer to the Appendix. \square

Note that the channel state information (CSI) required for setting the phase shift vectors \mathbf{u} and \mathbf{v} as per (12) and (13) is a b -bit quantized information of the phases of the source-relay and relay-destination channels, respectively. This b -bit quantized channel phase information can be acquired directly in the analog domain as per [15], [16], or by adapting any of the CSI acquisition methods developed for IRSs. In that sense, the relay system does not waste more resources in acquiring the CSI than the corresponding IRS system.

Corollary 1. *The rate in (14) is maximized to*

$$R_{\max} \approx \log_2 \left(1 + \frac{P_R^* \Omega_{RD} (1 + (N^* - 1)Q)}{N_0} \right), \quad (16)$$

where N^* and P_R^* are found from the following optimization problem

$$\begin{aligned} &\max_{P_R, N} R \\ &\text{s.t.} \quad M + N = K \\ &\quad P_S + P_R = P_T, \end{aligned} \quad (17)$$

where the objective function R is given in (14) and P_T is the total available power.

Proof. The rate in (14) can be maximized by optimizing N and P_R as per the optimization problem in (17). This will result in optimal N and P_R , denoted by N^* and P_R^* , that will make the two expressions in the min function in (14) equal. As a result, we can take any of the two expression in the $\min\{\cdot\}$ function in (14) with the optimal N^* and P_R^* found from (17) and thereby obtain the maximized rate in (16). \square

Corollary 2. *If instead of the FD mode, the relay works in the HD mode and uses all of its K antennas both for transmission*

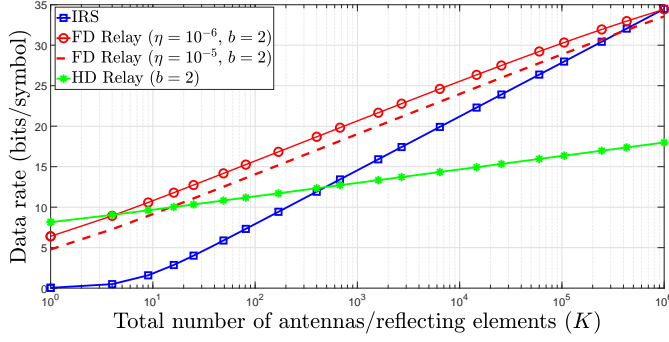


Fig. 2. Data rate as a function of the number of antenna elements K .

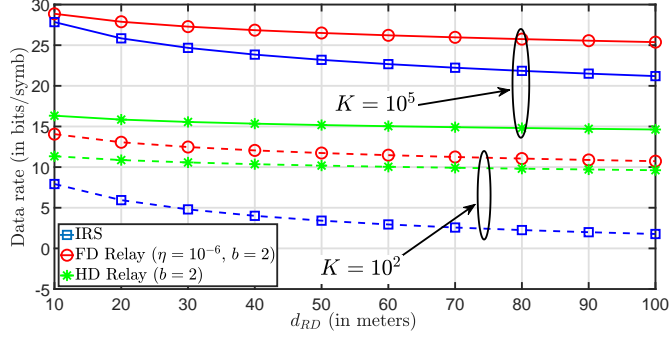


Fig. 3. Data rate as a function of the distance d_{RD} .

and reception in different time slots, the achieved rate of the corresponding HD relaying system would be

$$R_{HD} \approx \frac{\log_2 \left(1 + \frac{P_T \Omega_S (1 + (K-1)Q)}{N_0} \right) \log_2 \left(1 + \frac{P_T \Omega_D (1 + (K-1)Q)}{N_0} \right)}{\log_2 \left(1 + \frac{P_T \Omega_S (1 + (K-1)Q)}{N_0} \right) + \log_2 \left(1 + \frac{P_T \Omega_D (1 + (K-1)Q)}{N_0} \right)}. \quad (18)$$

Proof. The proof is straightforward using the vast available literature on HD relaying, e.g. [17]. \square

IV. NUMERICAL RESULTS

In this section, we compare the data rate achieved using the proposed FD relay for $b = 2$, given by (16) in Corollary 1, and the data rate achieved by an ideal IRS, given by [8, Eq. (48)]

$$R_{IRS} \approx \log_2 \left(1 + \frac{K^2 P_T \Omega_S \Omega_D}{N_0} \right). \quad (19)$$

As a benchmark, we also show the rate achieved by the HD relay, given by² (18).

The three rates are compared in Fig. 2 as a function of the total number of antenna elements K , when $\lambda = 0.1\text{m}$, $A = (\lambda/4)^2$, $d_{SR} = 25\text{m}$, $\alpha_{SR} = \pi/6$, $d_{RD} = 10\text{m}$, and $\alpha_{RD} = -\pi/6$. The total transmit power is $P_T = 1\text{W}$ while the thermal noise power is set to $N_0 = 10^{-12}\text{W}$. Each analog phase shifter at the relay is a 2-bit phase shifter, i.e., it can shift the phase

²We note that in the far-field regime the approximate rates given by (16), (18), and (19) are extremely accurate even for small K and their accuracy only improves as K grows.

by any of the following values $\mathcal{P} = \{0, \frac{\pi}{2}, \pi, \frac{3\pi}{2}\}$. As can be seen from Fig. 2, the FD relay significantly outperforms the IRS when the passive self-interference is either $\eta = 10^{-5}$ (i.e., 50 dB) or $\eta = 10^{-6}$ (i.e., 50 dB). When K becomes $K = 10^6$ or larger, the destination starts to operate in the near field of the relay/IRS, in which case it can be considered that the relay/IRS is a part of the destination. Moreover, in that range, the IRS does not outperform the FD relay, instead the two have identical performances since both can be considered as a part of the destination.

Fig. 3 compares the three data rates as a function of d_{RD} when $d_{SR} = 25\text{m}$ and the same parameters as for Fig. 2 are used. Two sets of curves are present, one for $K = 10^2$ and the other for $K = 10^5$ antenna elements. In both cases, the proposed FD relay significantly outperforms both the IRS and the HD relay.

V. CONCLUSION

We have proposed a single RF-chain multi-antenna FD relay that employs passive self-interference cancellation. Next, we have compared the data rate of a system comprised of a source, the proposed FD relay, and a destination with the data rate of the same system but with the FD relay replaced by an ideal IRS. We have shown that the FD relaying system with 2-bit quantized analog phase shifters significantly outperforms the IRS system.

APPENDIX

As a result of (10), the signal-to-interference-plus-noise ratio (SINR) at the receive-side of the relay, denoted by γ_{SR} , is given by

$$\gamma_{SR} = \frac{E_{x_S} \{ |x_S \mathbf{u}^T \mathbf{h}_S|^2 \}}{E_{\mathbf{w}_R} \{ |\mathbf{u}^T \mathbf{w}_R|^2 \} + E_{x_R, \mathbf{G}} \left\{ \left| \sqrt{\frac{1}{N}} x_R \mathbf{u}^T \mathbf{G} \mathbf{v} \right|^2 \right\}}, \quad (20)$$

where the subscript of the expectations indicates the random variable(s) with respect to which expectation is calculated. Now, we have

$$E_{x_S} \{ |x_S \mathbf{u}^T \mathbf{h}_S|^2 \} = P_S |\mathbf{u}^T \mathbf{h}_S|^2, \quad (21)$$

which follows since $E_{x_S} \{ |x_S|^2 \} = P_S$. Next, $|\mathbf{u}^T \mathbf{h}_S|^2$, when M is large, is given by

$$\begin{aligned} |\mathbf{u}^T \mathbf{h}_S|^2 &= \left| \sum_{m=1}^M \sqrt{\Omega_{SR}} e^{j\phi_{SR,m}} e^{-j\bar{\phi}_{SR,m}} \right|^2 \\ &= \left| \sum_{m=1}^M \sqrt{\Omega_{SR}} e^{j(\phi_{SR,m} - \bar{\phi}_{SR,m})} \right|^2 = \left| \sum_{m=1}^M \sqrt{\Omega_{SR}} e^{j\bar{\phi}_{SR,m}} \right|^2 \\ &= \sum_{m=1}^M \Omega_{SR} + \Omega_{SR} \sum_{m=1}^M \sum_{j=1, j \neq m}^M e^{j\bar{\phi}_{SR,m}} e^{-j\bar{\phi}_{SR,j}} \\ &= M \Omega_{SR} + M(M-1) \Omega_{SR} \sum_{m=1}^M \sum_{j=1, j \neq m}^M \frac{e^{j\bar{\phi}_{SR,m}} e^{-j\bar{\phi}_{SR,j}}}{M(M-1)} \\ &\approx M \Omega_{SR} + M(M-1) \Omega_{SR} E_j \{ e^{j\bar{\phi}_{SR,m}} \} E_j \{ e^{-j\bar{\phi}_{SR,j}} \} \\ &\stackrel{(b)}{=} M \Omega_{SR} + M(M-1) \Omega_{SR} \left(\frac{2^b}{\pi} \sin \left(\frac{\pi}{2^b} \right) \right)^2, \end{aligned} \quad (22)$$

where $\bar{\phi}_{SR,m} = \phi_{SR,m} - \hat{\phi}_{SR,m}$, and (b) follows from the fact that $\phi_{SR,m}$ and $\phi_{SR,j}$ have uniform distributions over $[-\frac{\pi}{2^b}, \frac{\pi}{2^b}]$. Moreover, $E_{\mathbf{w}_R} \{ |\mathbf{u}^T \mathbf{w}_R|^2 \}$ is given by

$$E_{\mathbf{w}_R} \{ |\mathbf{u}^T \mathbf{w}_R|^2 \} = MN_0. \quad (23)$$

Lastly, the average power of the self-interference is given by

$$E_{x_R, \mathbf{G}} \left\{ \left| \sqrt{\frac{1}{N}} x_R \mathbf{u}^T \mathbf{G} \mathbf{v} \right|^2 \right\} \stackrel{(c)}{=} \frac{P_R}{N} E_{\mathbf{G}} \{ |\mathbf{u}^T \mathbf{G} \mathbf{v}|^2 \}, \quad (24)$$

where (c) results from $E_{x_R} \{ |x_R|^2 \} = P_R$. On the other hand, $E_{\mathbf{G}} \{ |\mathbf{u}^T \mathbf{G} \mathbf{v}|^2 \}$ is obtained as

$$\begin{aligned} E_{\mathbf{G}} \{ |\mathbf{u}^T \mathbf{G} \mathbf{v}|^2 \} &= E_{\mathbf{G}} \left\{ \left| \sum_{m=1}^M \sum_{n=1}^N g_{mn} e^{-j\hat{\phi}_{SR,m}} e^{-j\hat{\phi}_{RD,n}} \right|^2 \right\} \\ &= E_{\mathbf{G}} \left\{ \sum_{m=1}^M \sum_{n=1}^N |g_{mn}|^2 + \sum_{m=1}^M \sum_{n=1}^N \sum_{i=1, i \neq m}^M \sum_{j=1, j \neq n}^N g_{mn} g_{ij} \right. \\ &\quad \times e^{-j\hat{\phi}_{SR,m}} e^{-j\hat{\phi}_{RD,n}} e^{j\hat{\phi}_{SR,i}} e^{j\hat{\phi}_{RD,j}} \left. \right\} \\ &= \sum_{m=1}^M \sum_{n=1}^N E_{\mathbf{G}} \{ |g_{mn}|^2 \} \\ &\quad + \sum_{m=1}^M \sum_{n=1}^N \sum_{i=1, i \neq m}^M \sum_{j=1, j \neq n}^N E_{\mathbf{G}} \{ g_{mn} \} E_{\mathbf{G}} \{ g_{ij} \} \\ &\quad \times e^{-j\hat{\phi}_{SR,m}} e^{-j\hat{\phi}_{RD,n}} e^{j\hat{\phi}_{SR,i}} e^{j\hat{\phi}_{RD,j}} \\ &= \sum_{m=1}^M \sum_{n=1}^N E_{\mathbf{G}} \{ |g_{mn}|^2 \} = MN\sigma_I^2 \stackrel{(d)}{=} N\eta, \end{aligned} \quad (25)$$

where (d) follows when (8) holds with equality. Inserting (25) into (24), we obtain (24) as

$$E_{x_R, \mathbf{G}} \left\{ \left| \sqrt{\frac{1}{N}} x_R \mathbf{u}^T \mathbf{G} \mathbf{v} \right|^2 \right\} = P_R\eta. \quad (26)$$

Now, combining (26), (23), (21), and (22) into (20), we obtain γ_{SR} as

$$\gamma_{SR} \approx \frac{P_S \left(\Omega_{SR} + (M-1)\Omega_{SR} \left(\frac{2^b}{\pi} \sin \left(\frac{\pi}{2^b} \right) \right)^2 \right)}{N_0 + \frac{\eta}{M} P_R}. \quad (27)$$

On the other hand, from (11), the received signal-to-noise ratio (SNR) at the destination, denoted by γ_{RD} , is given by

$$\gamma_{RD} = \frac{E_{x_R} \left\{ \left| \frac{1}{\sqrt{N}} x_R \mathbf{v}^T \mathbf{h}_D \right|^2 \right\}}{E_{w_D} \{ w_D^2 \}} \stackrel{(e)}{=} \frac{P_R |\mathbf{v}^T \mathbf{h}_D|^2}{NN_0}, \quad (28)$$

where (e) results from $E\{ |x_R^2| \} = P_R$. In (28), $|\mathbf{v}^T \mathbf{h}_D|^2$ can be obtained by replacing N with M and Ω_{RD} with Ω_{SR} in (22). As a result, γ_{RD} is given by

$$\gamma_{RD} \approx \frac{P_R \left(\Omega_{RD} + (N-1)\Omega_{RD} \left(\frac{2^b}{\pi} \sin \left(\frac{\pi}{2^b} \right) \right)^2 \right)}{N_0}. \quad (29)$$

Finally, the the achievable rate is given by

$$R = \min \{ \log_2 (1 + \gamma_{SR}), \log_2 (1 + \gamma_{RD}) \}, \quad (30)$$

where γ_{SR} and γ_{RD} are given in (27) and (29), respectively, which leads to (14).

REFERENCES

- [1] C. Liaskos, S. Nie, A. Tsoliaridou, A. Pitsillides, S. Ioannidis, and I. Akyildiz, "A new wireless communication paradigm through software-controlled metasurfaces," *IEEE Communications Magazine*, vol. 56, no. 9, pp. 162–169, 2018.
- [2] Q. Wu and R. Zhang, "Towards smart and reconfigurable environment: Intelligent reflecting surface aided wireless network," *IEEE Communications Magazine*, vol. 58, no. 1, pp. 106–112, 2020.
- [3] M. Di Renzo, K. Ntontin, J. Song, F. H. Danufane, X. Qian, F. Lazarakis, J. De Rosny, D. T. Phan-Huy, O. Simeone, R. Zhang, M. Debbah, G. Leroay, M. Fink, S. Tretyakov, and S. Shamai, "Reconfigurable intelligent surfaces vs. relaying: Differences, similarities, and performance comparison," *IEEE Open Journal of the Communications Society*, vol. 1, pp. 798–807, 2020.
- [4] E. Björnson, . Özdogan, and E. G. Larsson, "Intelligent reflecting surface versus decode-and-forward: How large surfaces are needed to beat relaying?" *IEEE Wireless Communications Letters*, vol. 9, no. 2, pp. 244–248, 2020.
- [5] K. Ntontin, M. Di Renzo, and F. Lazarakis, "On the rate and energy efficiency comparison of reconfigurable intelligent surfaces with relays," in *2020 IEEE 21st International Workshop on Signal Processing Advances in Wireless Communications (SPAWC)*, 2020, pp. 1–5.
- [6] A. F. Molisch, V. V. Ratnam, S. Han, Z. Li, S. L. H. Nguyen, L. Li, and K. Haneda, "Hybrid beamforming for massive mimo: A survey," *IEEE Communications Magazine*, vol. 55, no. 9, pp. 134–141, 2017.
- [7] I. Ahmed, H. Khammar, A. Shahid, A. Musa, K. S. Kim, E. De Poorter, and I. Moerman, "A survey on hybrid beamforming techniques in 5g: Architecture and system model perspectives," *IEEE Communications Surveys Tutorials*, vol. 20, no. 4, pp. 3060–3097, 2018.
- [8] E. Björnson and L. Sanguinetti, "Power scaling laws and near-field behaviors of massive mimo and intelligent reflecting surfaces," *IEEE Open Journal of the Communications Society*, vol. 1, pp. 1306–1324, 2020.
- [9] R. Méndez-Rial, C. Rusu, N. González-Prelcic, A. Alkhateeb, and R. W. Heath, "Hybrid mimo architectures for millimeter wave communications: Phase shifters or switches?" *IEEE Access*, vol. 4, pp. 247–267, 2016.
- [10] E. J. Black, "Holographic beam forming and mimo," *Pivotal Commware, unpublished*, 2017.
- [11] A. Pizzo, T. L. Marzetta, and L. Sanguinetti, "Spatially-stationary model for holographic mimo small-scale fading," *IEEE Journal on Selected Areas in Communications*, vol. 38, no. 9, pp. 1964–1979, 2020.
- [12] N. Zlatanov, E. Sippel, V. Jamali, and R. Schober, "Capacity of the gaussian two-hop full-duplex relay channel with residual self-interference," *IEEE Transactions on Communications*, vol. 65, no. 3, pp. 1005–1021, 2017.
- [13] E. Everett, A. Sahai, and A. Sabharwal, "Passive self-interference suppression for full-duplex infrastructure nodes," *IEEE Transactions on Wireless Communications*, vol. 13, no. 2, pp. 680–694, 2014.
- [14] D. Korpi, M. Heino, C. Icheln, K. Haneda, and M. Valkama, "Compact inband full-duplex relays with beyond 100 db self-interference suppression: Enabling techniques and field measurements," *IEEE Transactions on Antennas and Propagation*, vol. 65, no. 2, pp. 960–965, 2017.
- [15] V. V. Ratnam and A. F. Molisch, "Periodic analog channel estimation aided beamforming for massive mimo systems," *IEEE Transactions on Wireless Communications*, vol. 18, no. 3, pp. 1581–1594, 2019.
- [16] ———, "Continuous analog channel estimation-aided beamforming for massive mimo systems," *IEEE Transactions on Wireless Communications*, vol. 18, no. 12, pp. 5557–5570, 2019.
- [17] N. Zlatanov, R. Schober, and P. Popovski, "Buffer-aided relaying with adaptive link selection," *IEEE Journal on Selected Areas in Communications*, vol. 31, no. 8, pp. 1530–1542, 2013.